United Nations Educational, Scientific and Cultural Organization

UNESCO Chair on the Prevention and Sustainable Management of Geo-Hydrological Hazards, University of Florence, Italy

Application of landslide science in practice

Examples from Italy

Nicola Casagli

Landslides

Slides may occur in almost every conceivable manner, slowly and suddenly, and with or without any apparent provocation

From: Terzaghi K., & Peck R.B. *(1967)* - *Soil mechanics in engineering practice.* 2nd edition.

Ralph Peck and Karl Terzaghi
at Lake Maracaibo in 1956
(From The Terzaghi & Peck Libraries NGI, Oslo)

Landslide risk in numbers

Areas at landslide risk
ca. 2 million landslides
ca. 10.000 areas at high landslide risk

Social impact (100 years)
ca. 4000 events affecting people
12.600 casualties
700.000 homeless

Economic impact (per year)
ca. 2 billion Euro of direct loss (0.1% of GDP)
ca. 4 - 5 billion Euro of indirect loss (0.1% of GDP)

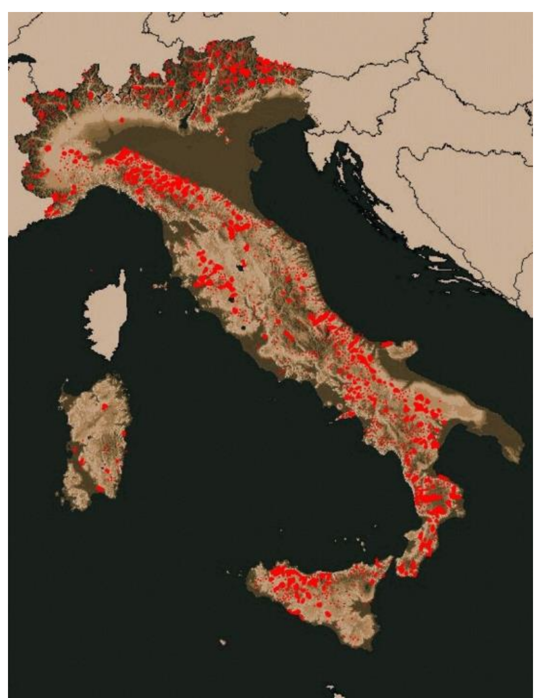

Landslide classification

Table 5 Summary of the proposed new version of the Varnes classification system. The words in italics are placeholders (use only one)

Type of movement	Rock	Soil
Fall	1. *Rock/ice* fall[a]	2. *Boulder/debris/silt* fall[a]
Topple	3. Rock block topple[a]	5. *Gravel/sand/silt* topple[a]
	4. Rock flexural topple	
Slide	6. Rock rotational slide	11. *Clay/silt* rotational slide
	7. Rock planar slide[a]	12. *Clay/silt* planar slide
	8. Rock wedge slide[a]	13. *Gravel/sand/debris* slide[a]
	9. Rock compound slide	14. *Clay/silt* compound slide
	10. Rock irregular slide[a]	
Spread	15. Rock slope spread	16. *Sand/silt* liquefaction spread[a]
		17. Sensitive clay spread[a]
Flow	18. *Rock/ice* avalanche[a]	19. *Sand/silt/debris* dry flow
		20. *Sand/silt/debris* flowslide[a]
		21. Sensitive clay flowslide[a]
		22. Debris flow[a]
		23. Mud flow[a]
		24. Debris flood
		25. Debris avalanche[a]
		26. Earthflow
		27. Peat flow
Slope deformation	28. Mountain slope deformation	30. Soil slope deformation
	29. Rock slope deformation	31. Soil creep
		32. Solifluction

For formal definitions of the landslide types, see text of the paper.

[a] Movement types that usually reach extremely rapid velocities as defined by Cruden and Varnes (1996). The other landslide types are most often (but not always) extremely slow to very rapid

Hungr et al. (2014)

Simple landslide classification

Rapid long runout landslides
Caused by earthquakes and heavy rainfalls

Characteristics
- Rapid Motion
- Great Impact Force
- Wide Disaster Area

Great number of death

	Rapid - velocity - Slow	
Long run-out distance	Rapid long run-out landslides (liquefied slides, etc)	slow long - traveling landslides (Earth flows, etc)
short-moving landslides	Rapid short-moving landslides (first-time slides)	Slow short - moving landslides (reactivated landslides)

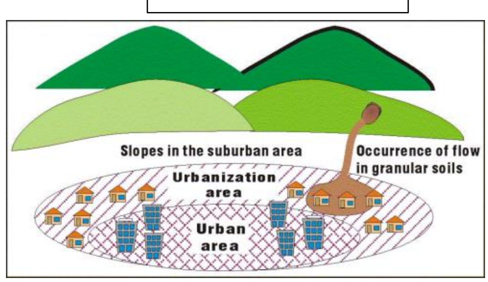

Kyoji Sassa (2001)

Velocity

Table 2 Landslide velocity scale (WP/WLI 1995 and Cruden and Varnes 1996)

Velocity class	Description	Velocity (mm/s)	Typical velocity	Response[a]
7	Extremely rapid	5×10^{3}	5 m/s	Nil
6	Very rapid	5×10^{1}	3 m/min	Nil
5	Rapid	5×10^{-1}	1.8 m/h	Evacuation
4	Moderate	5×10^{-3}	13 m/month	Evacuation
3	Slow	5×10^{-5}	1.6 m/year	Maintenance
2	Very slow	5×10^{-7}	16 mm/year	Maintenance
1	Extremely Slow			Nil

[a] Based on Hungr (1981)

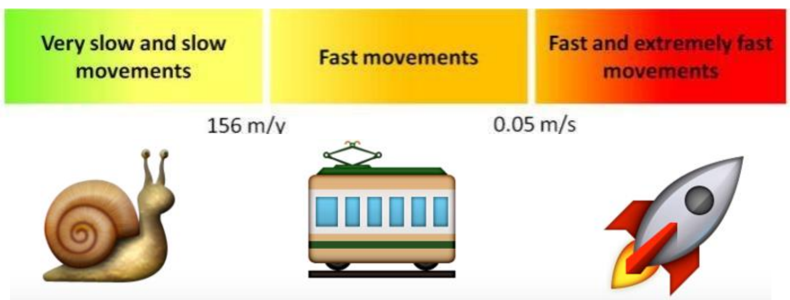

Creep Law

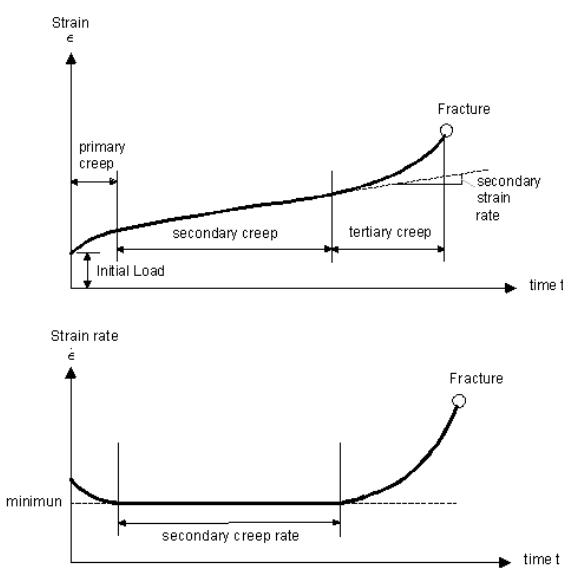

Apollonius of Perga

(Perga, 262 a.C. – Murtina, 190 a.C.)

The conics

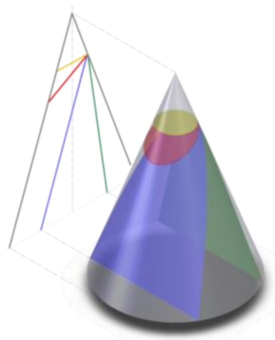

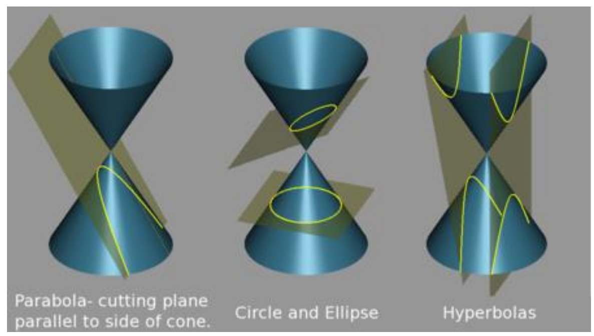

Forecasting time of failure

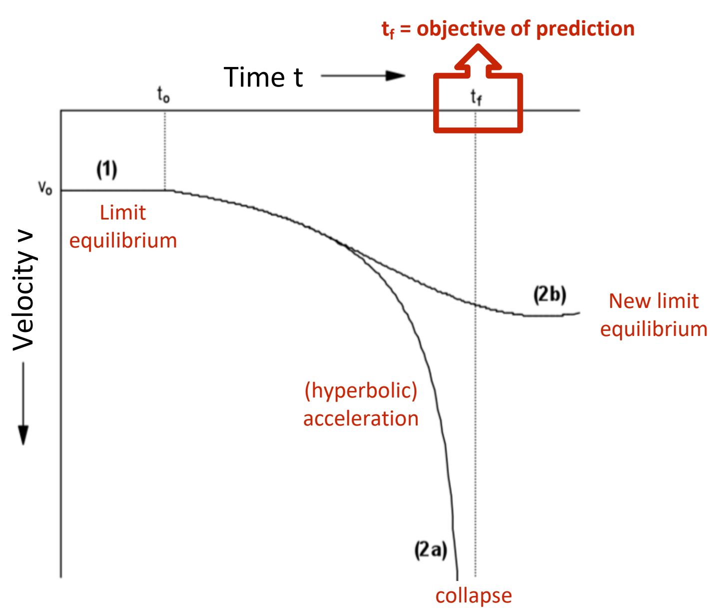

Saito (1965)

- Forecasting method of the the time of failure based on creep law
- Hyperbolic acceleration before collapse
- Linear relationship between the inverse velocity and the time of failure

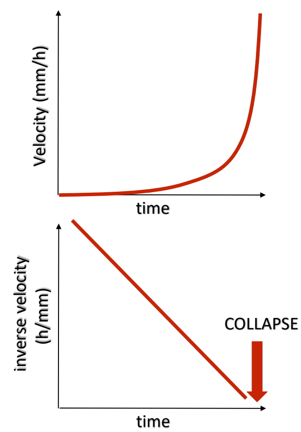

Inverse velocity method Fukuzono (1985)

$$\frac{d^2x}{dt^2} = A\left(\frac{dx}{dt}\right)^{\alpha}$$

If $\alpha = 2$ then $V^{-1} = A(t_f - t)$: HYPERBOLA

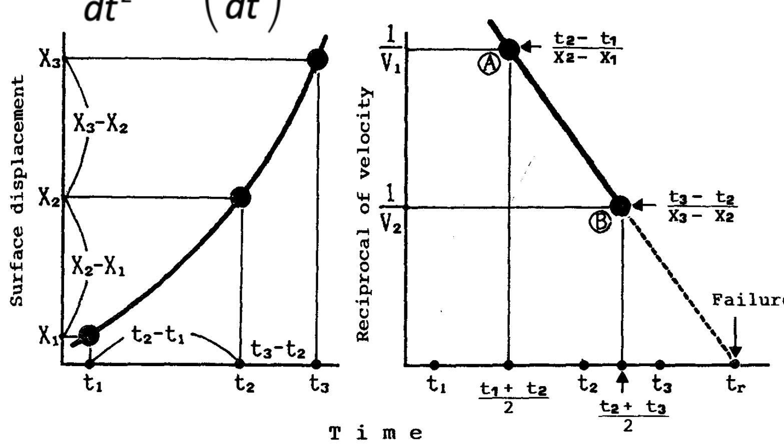

Barry Voight (1988)

A relation to describe rate-dependent material failure. Science (1988)

A method for prediction of volcano eruptions. Nature (1988)

Barry Voight and Discovery Channel film crew, the devastated city of Plymouth, Montserrat, WI, May 2002

July 1995, Montserrat's Soufriere Hills volcano

Forecasting Vajont landslide collapse

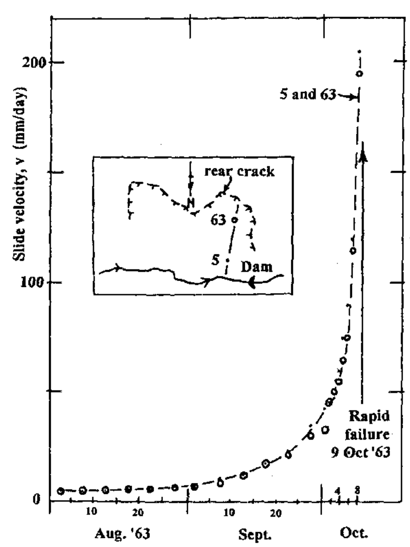

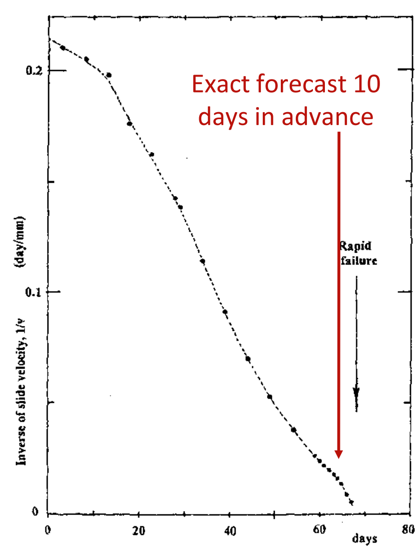

(Hutchinson, 2001)

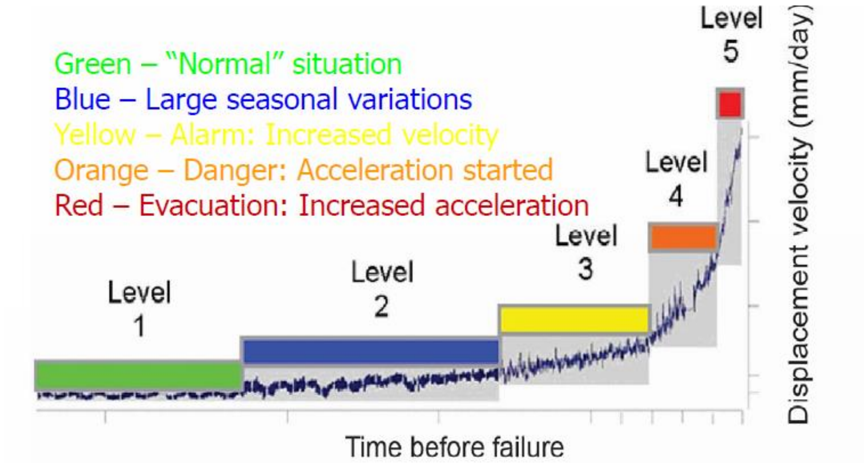

Blikra L.H., 2008. The Aknes rockslide. Monitoring, threshold values and early warning. 10th International Symposium on Landslides and Engineering Slopes, 30th June- 4th July, Xian, China, pp. 1089-1094.

NOTHING SPECIAL	**BE AWARE**	**BE PREPARED**	**TAKE ACTION**
Stable or constant velocity	Start of acceleration	Sustained acceleration	Asymptotic acceleration
Weekly reports	Daily reports	Hourly reports	Continuos reports

ELSEVIER

Engineering Geology
Volumes 147–148, 12 October 2012, Pages 124-136

Design and implementation of a landslide early warning system

Emanuele Intrieri, Giovanni Gigli, Francesco Mugnai, Riccardo Fanti, Nicola Casagli

Show more

https://doi.org/10.1016/j.enggeo.2012.07.017

Motorway A6

Earth slide debris flow

Rapid long runout

GB-InSAR

A6 Savona-Torino 24/11/2019


10:49 Gio 28 nov
99%
A6
A6 Torino - Savona
E717
E717
A6 Torino - Savona
E717
del Monte
Via N. S. del Monte
Madonna del Monte
Chiesa di Madonna del monte
Forte Madonna del Monte 1883
Google

Viaduct Madonna del Monte

Viaduct

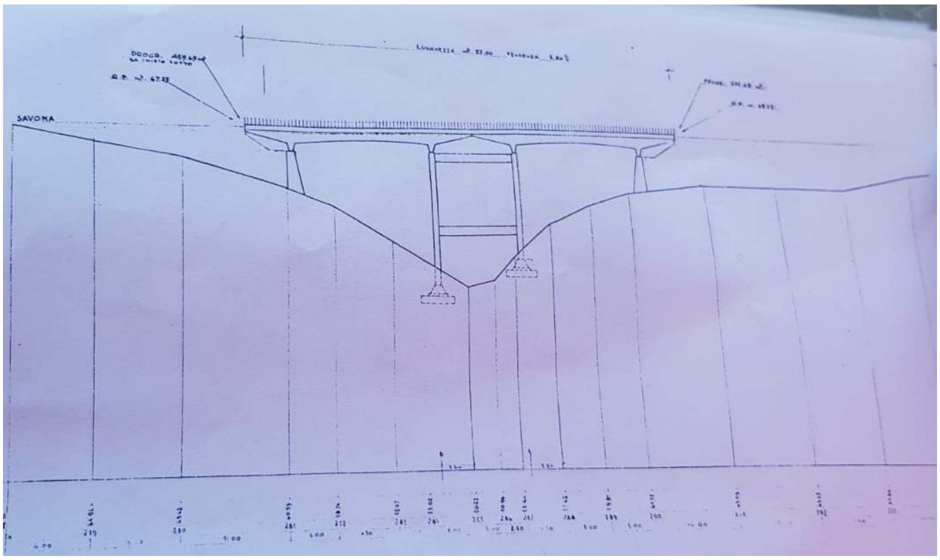
SAVONA

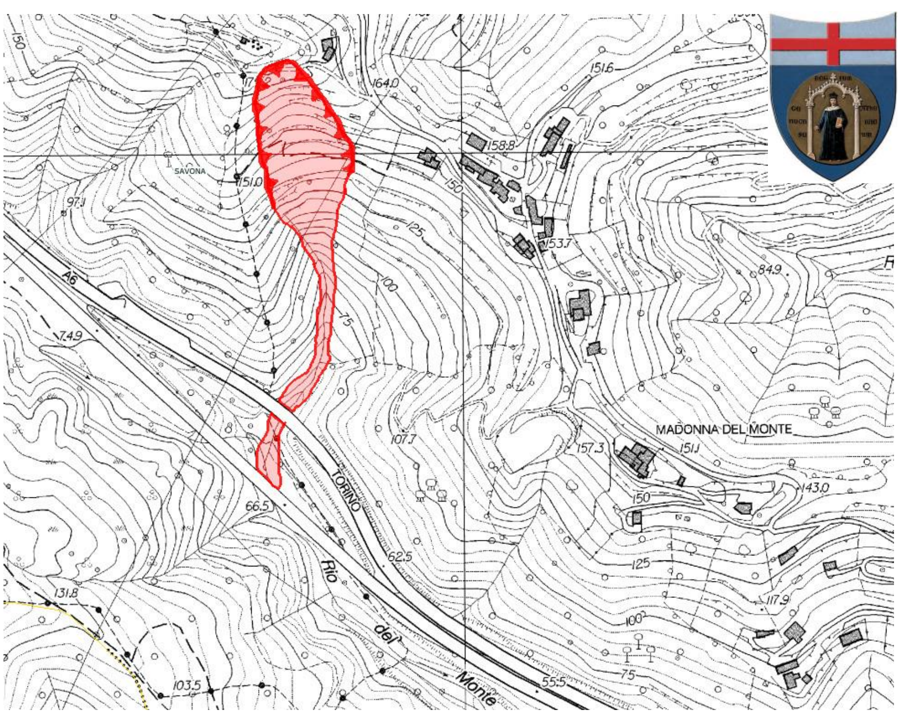
150
164.0
151.6
158.8
SAVONA
151.0
97.1
125
153.7
84.9
100
75
A6
74.9
107.7
157.3
MADONNA DEL MONTE
151.1
143.0
150
TORINO
66.5
62.5
Rio
del
Monte
125
117.9
131.8
100
103.5
75
55.5

Landslide map

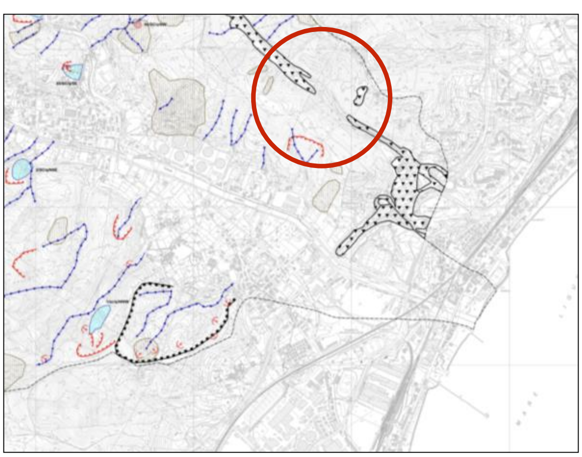

REGIONE LIGURIA

Landslide susceptibility

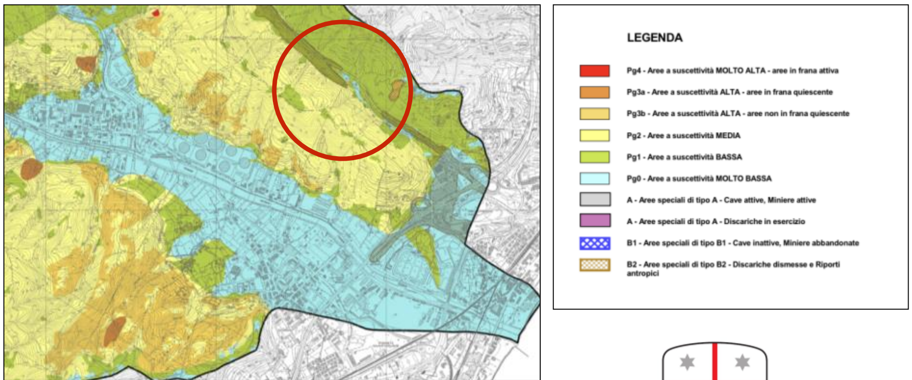

REGIONE LIGURIA

Risk map

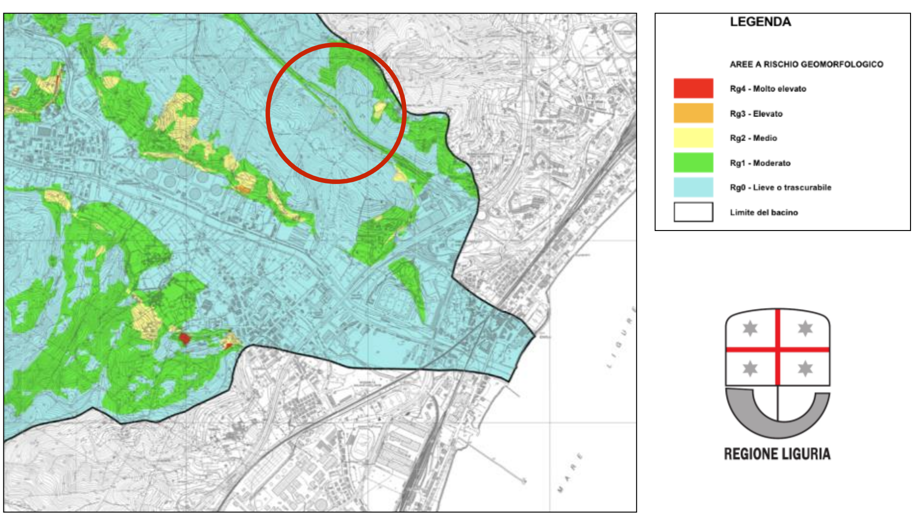

REGIONE LIGURIA

Watershed

Watershed

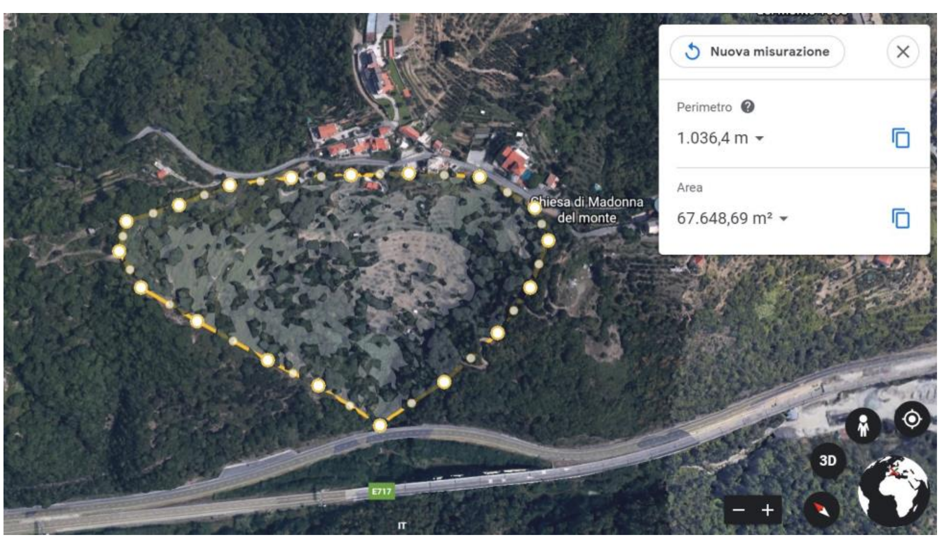

Watershed

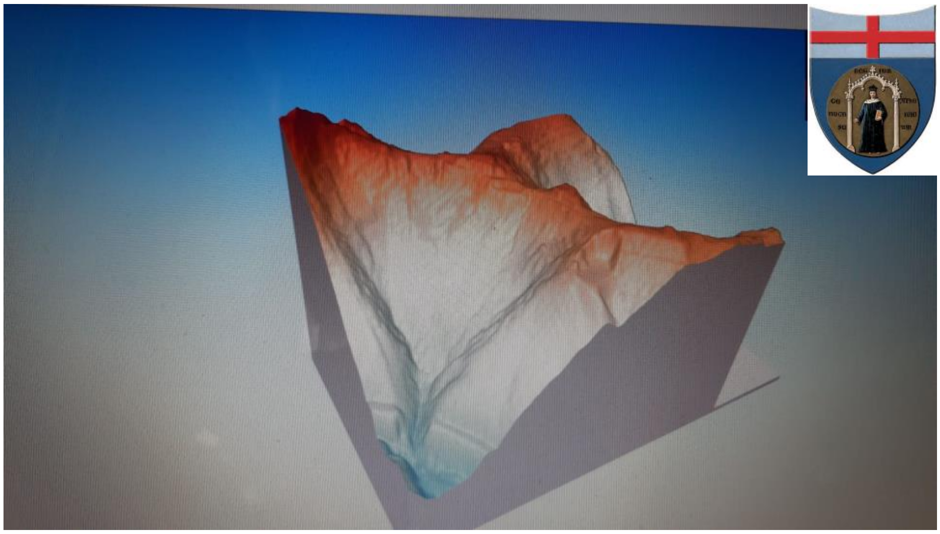

Last week rainfall

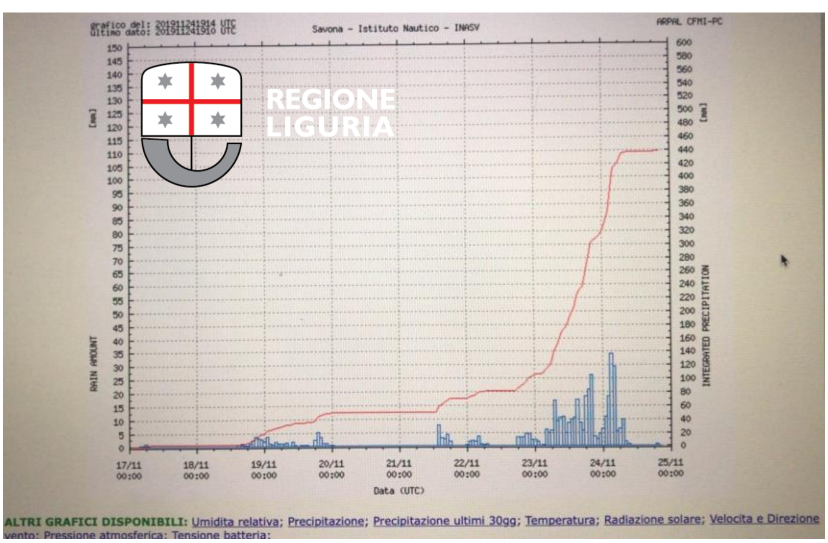

Last month rainfall

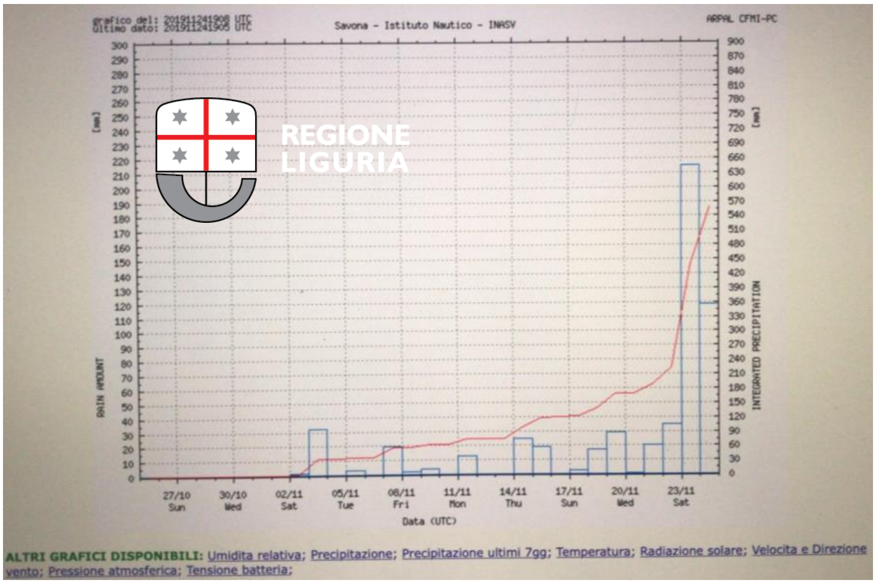

Ground-based InSAR LiSAMobile

Ground-based InSAR IBIS-FS

IDS
GeoRadar

Ground-based InSAR Hydra

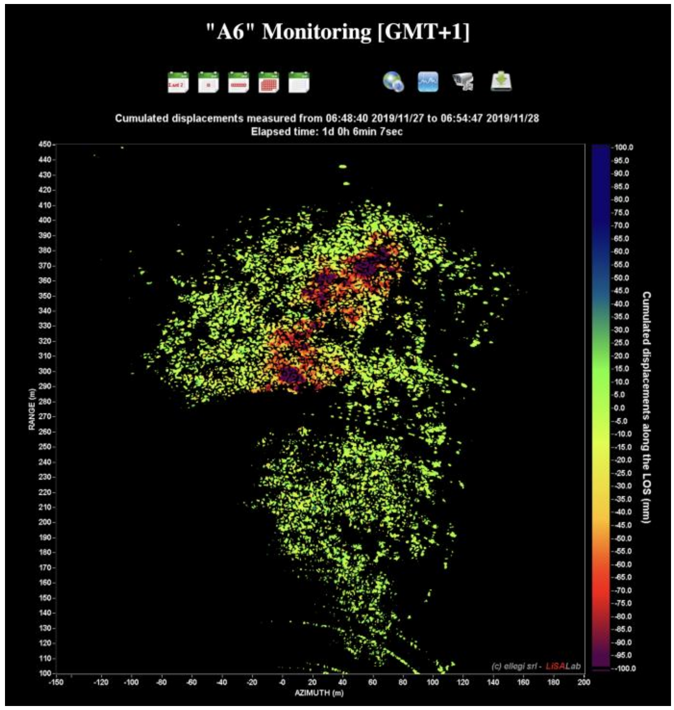

Cumultaed displacemennts

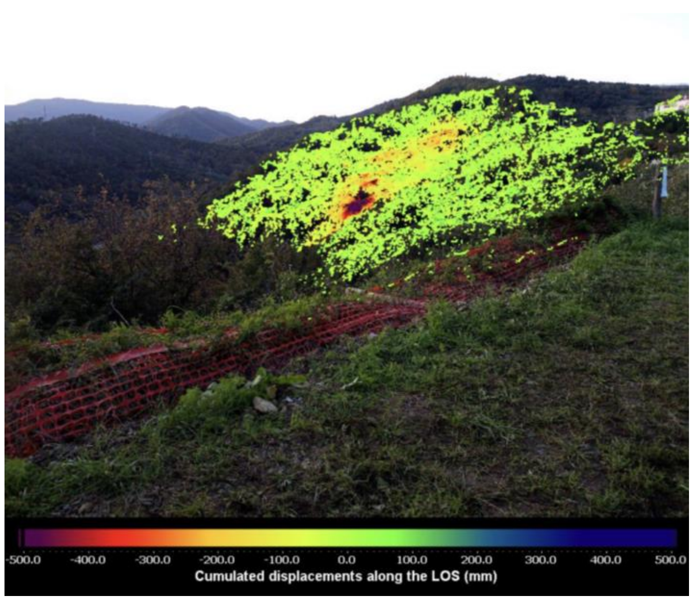

Time series

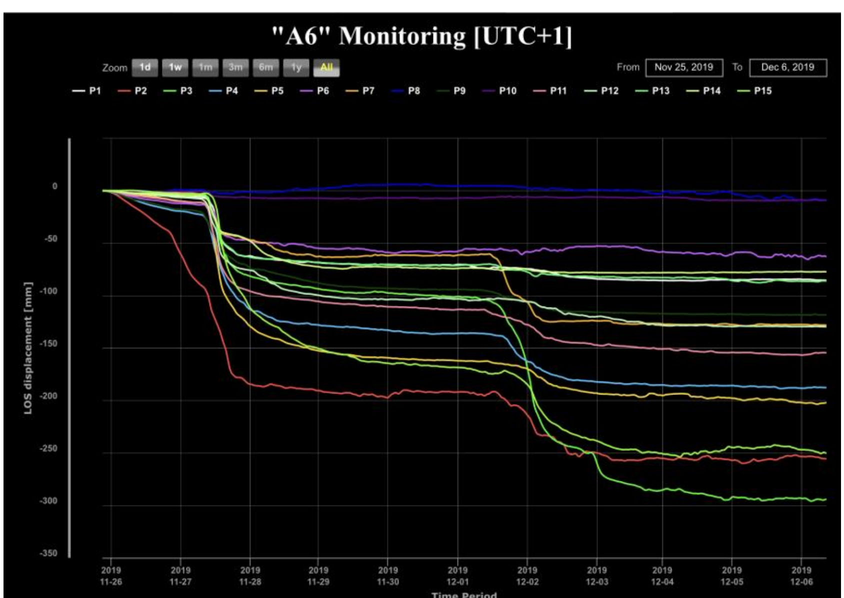
"A6" Monitoring [UTC+1]
Zoom 1d 1w 1m 3m 6m 1y All
From Nov 25, 2019 To Dec 6, 2019
P1 P2 P3 P4 P5 P6 P7 P8 P9 P10 P11 P12 P13 P14 P15
LOS displacement [mm]
0
-50
-100
-150
-200
-250
-300
-350
2019 11-26
2019 11-27
2019 11-28
2019 11-29
2019 11-30
2019 12-01
2019 12-02
2019 12-03
2019 12-04
2019 12-05
2019 12-06
Time Period

Pluviometer

Rainfall 27-28/11/2019

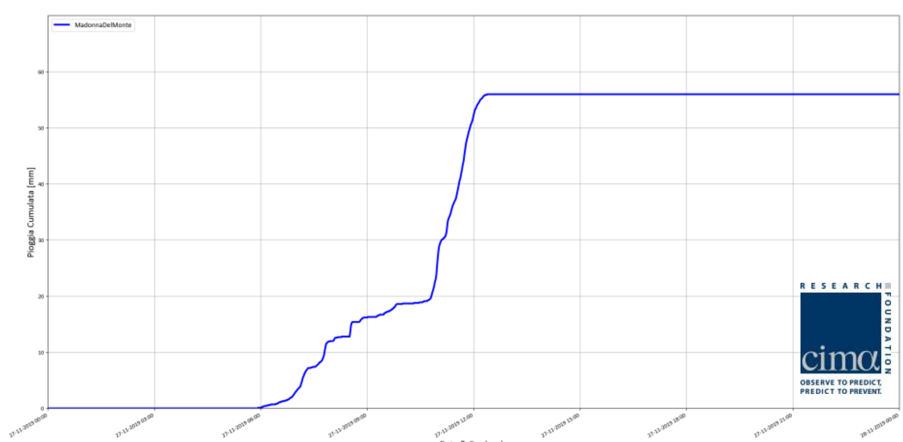

DMS

Strumenti per il monitoraggio geotecnico di stabilità di versanti, scavi e opere dell'ingegneria geotecnica

SCHEDA TECNICA

DMS-*i* SCOUT

Sensore inclinometrico triassiale	
Tipologia sensore	MEMS
Range	± 90°
Risoluzione	0.01°
Ripetitibilità	± 0.02°
Linearità	0.05% FS

Sensore piezometrico	
Tipologia sensore	Resistivo
Range	30 psi
Sensibilità	3.33 mV/psi
Risoluzione	0.02 psi
Ripetitibilità	0.05% FS
Linearità	± 0.05% FS

Sensore accelerometrico	
Tipologia sensore	MEMS 3 assi
Range	± 2 g
Sensibilità	0.001 mg/LSB
Livello di rumore	25 µg/√Hz

Sensore di temperatura	
Tipologia sensore	Termoresistenza al platino
Classe	A (DIN EN 60751/95)
Range	-50°C / +130°C
Resistenza	1 kΩ @0°C
Risoluzione	0.1°C
Tolleranza	± 0.15°C @0°C

DMS

Strumenti per il monitoraggio geotecnico di stabilità di versanti, scavi e opere dell'ingegneria geotecnica

SCHEDA TECNICA

DMS-*i* SCOUT

Monitoring system

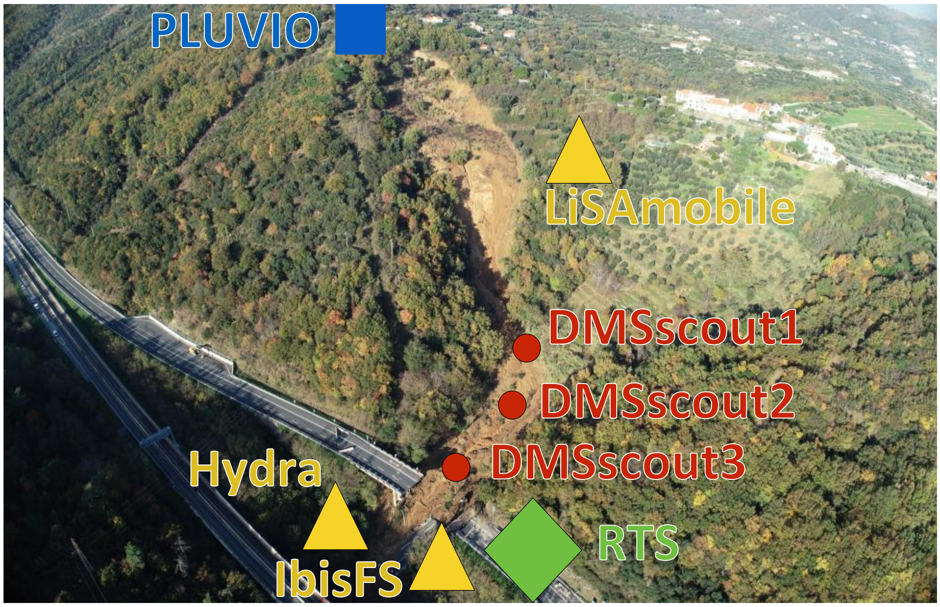

Alerts and tresholds

ALERT	Weather-based warning	Pluviometer	Ground-based radar monitoring	DMS	ALARM
NONE	GREEN	< treshold	< treshold	< treshold	**NONE**
ORDINARY	YELLOW	> treshold	> treshold	> treshold	**ATTENTION**
MODERATE	ORANGE	> treshold	> treshold	> treshold	**PREALARM**
HIGH	RED	> treshold	> treshold	> treshold	**ALARM**

Ground-based radar

Siti di monitoraggio

40+ monitoring sites

7 active now

Rockfall

Rapid short runout

GB-InSAR

Gallivaggio, 10 October 1492

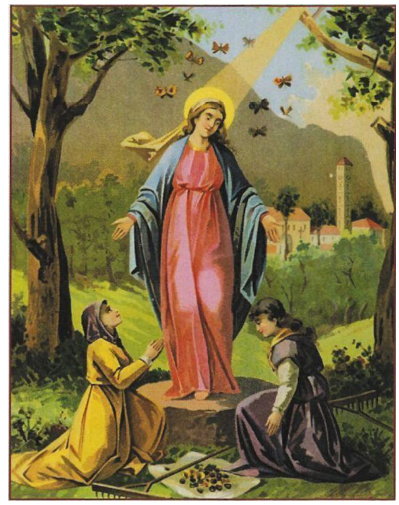

Our Lady Sanctuary

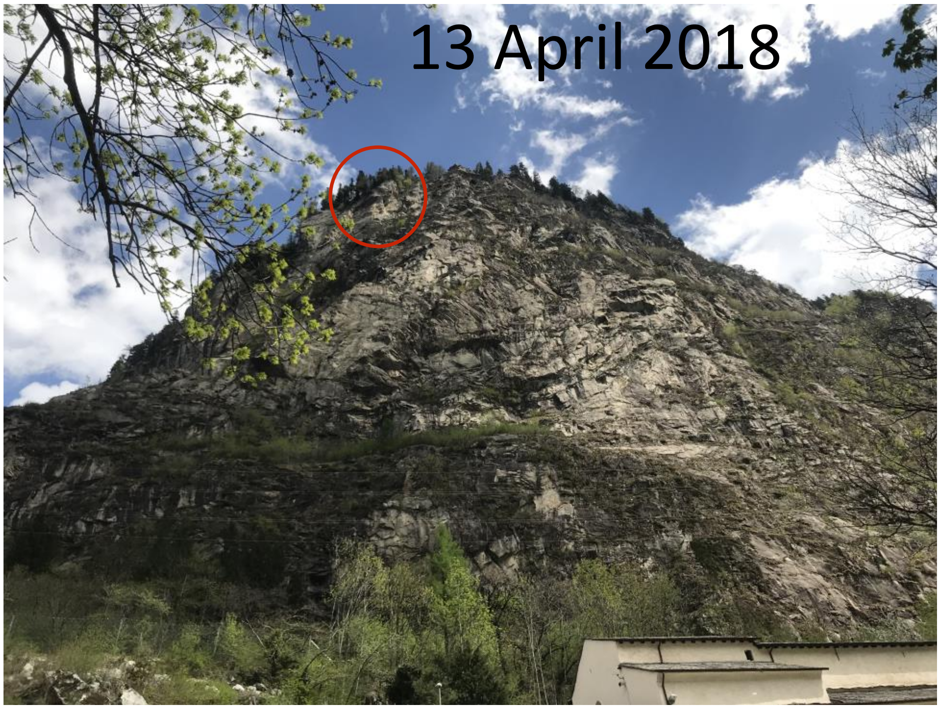
13 April 2018


26 April 2018

Radar monitoring

Radar monitoring

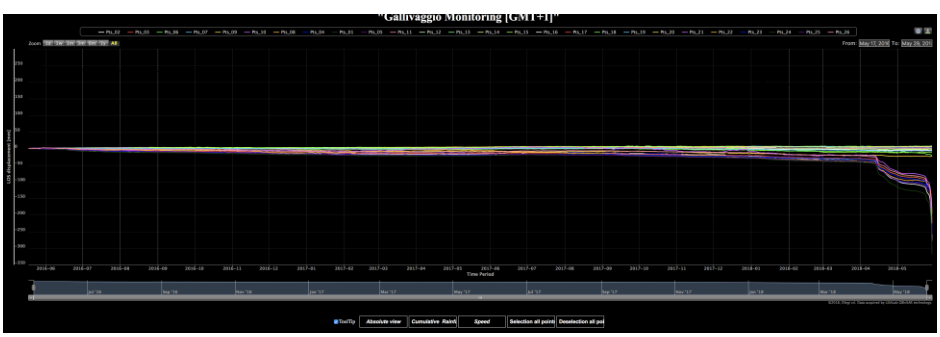

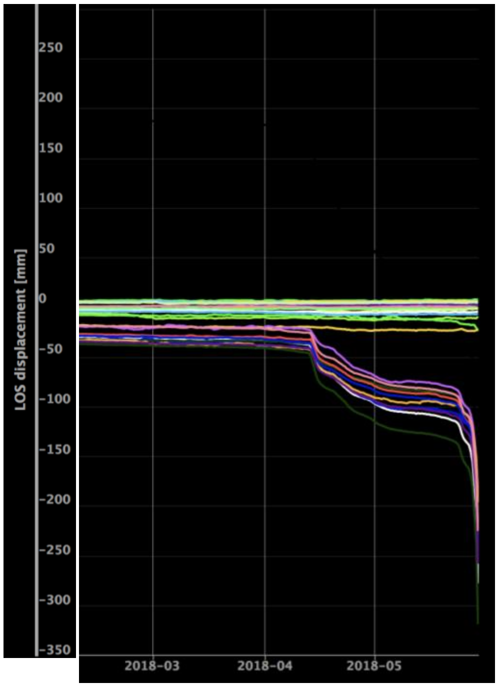

Collapse 29 May 2018 16:36

Collapse forecasting

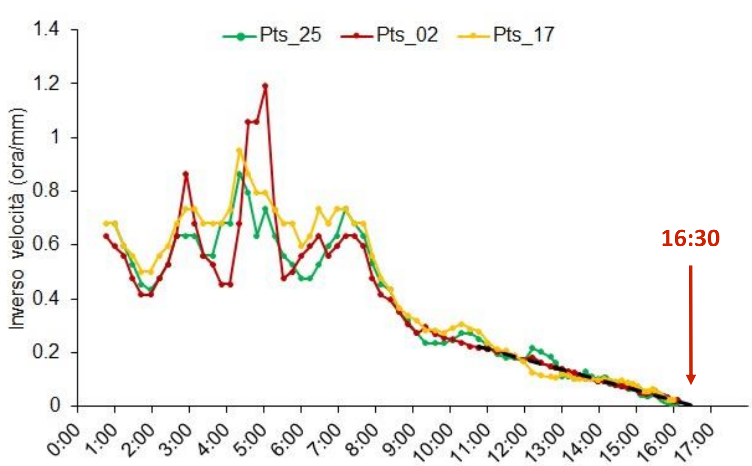

Gallivaggio 29 May 2018 16:36

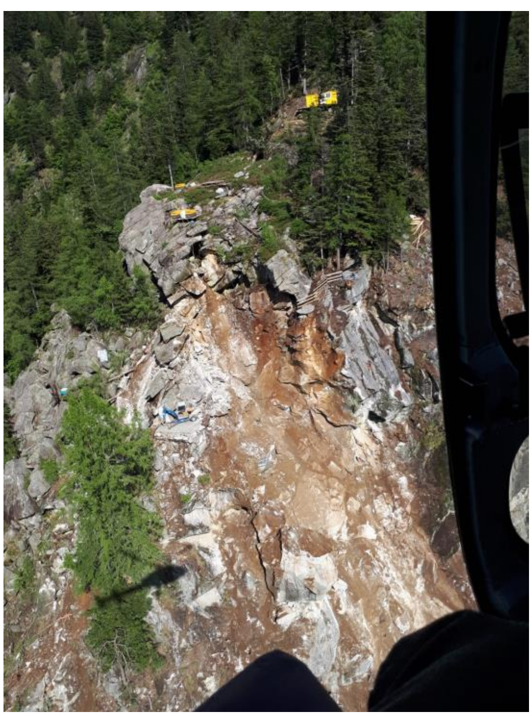

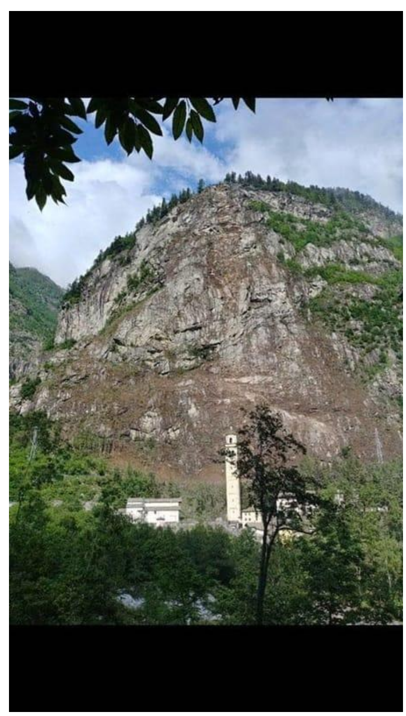

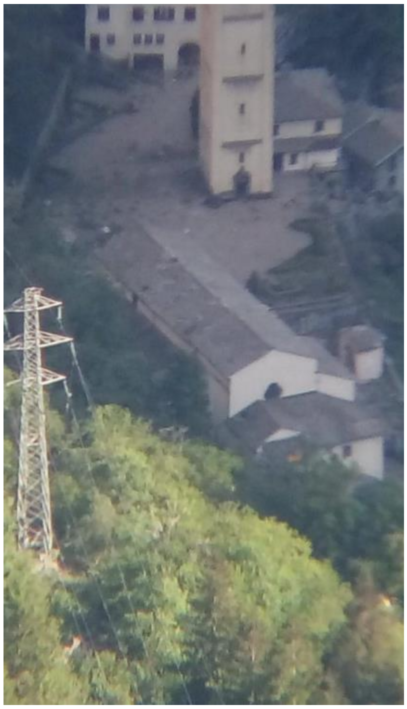

Zoom

SpringerLink

Landslides
August 2019, Volume 16, Issue 8, pp 1425–1435 | Cite as

Rockfall forecasting and risk management along a major transportation corridor in the Alps through ground-based radar interferometry

Authors | Authors and affiliations

Tommaso Carlà, Teresa Nolesini, Lorenzo Solari, Carlo Rivolta, Luca Dei Cas, Nicola Casagli

Open Access | Original Paper
First Online: 11 May 2019

1.3k Downloads 1 Citations

Radar satellites

Radar satellites


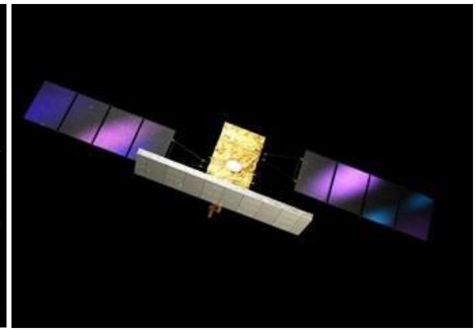

esa

sentinel-1

COSMO SkyMed KEEPING AN EYE ON THE WORLD

agenzia spaziale italiana

Persistent Scatterers Interferometry (PS)

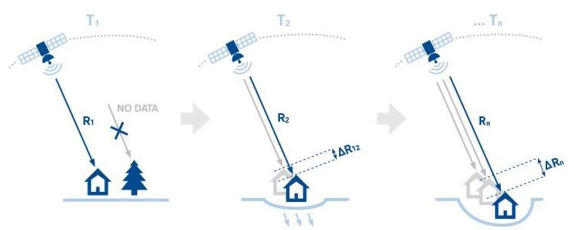

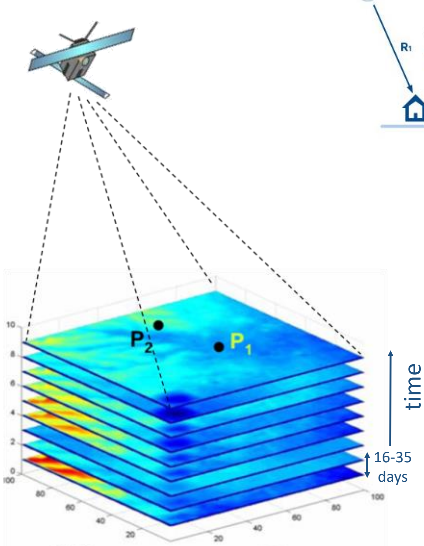

LOS average displacement rate

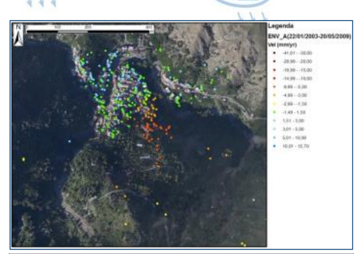

Deformation time series

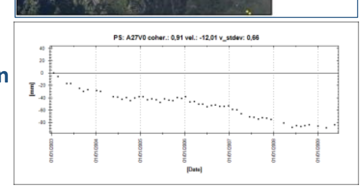

Applications

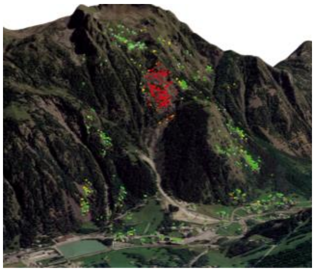

Landslides

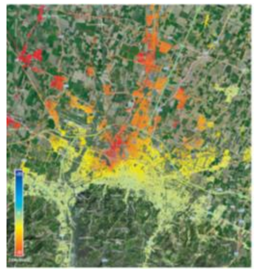

Subsidence

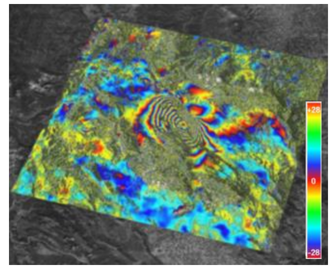

Tectonics

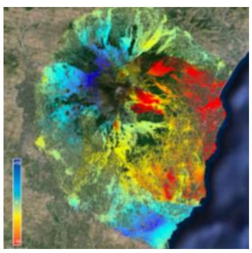

Volcanic activity

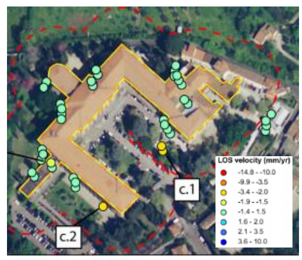

Buildings

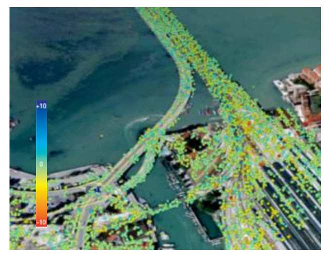

Infrastructures

National coverage PSI

22 million of permanent scatterers

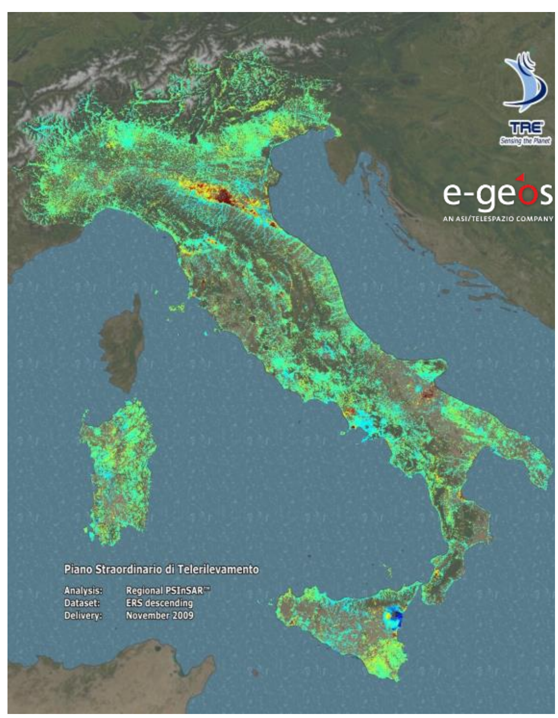

National PS coverages

PS Continous Streaming

sentinel

esa
European Space Agency

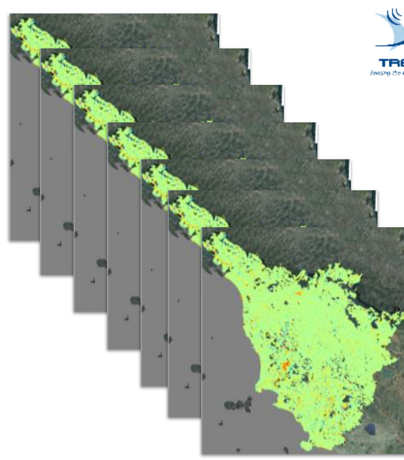

Revisiting time: 6 days

First application of PS-InSAR Continuous Streaming at regional scale (2016)

Regional PS Streaming

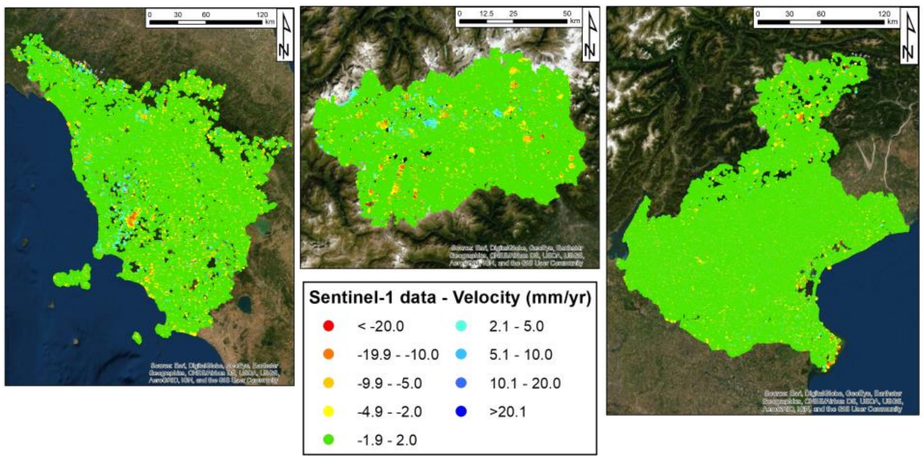

The Tuscany region

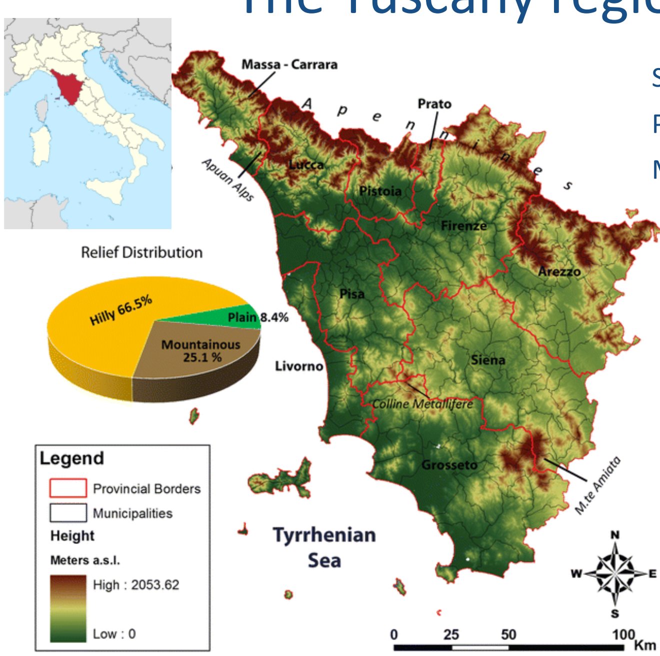

Surface = 22,987 km^2

Population = 3.7 million

Municipalities = 276

>90% of the territory is hilly of mountainous

90k landslides

390 landslides/100 km^2

Sentinel-1 archive since 2014

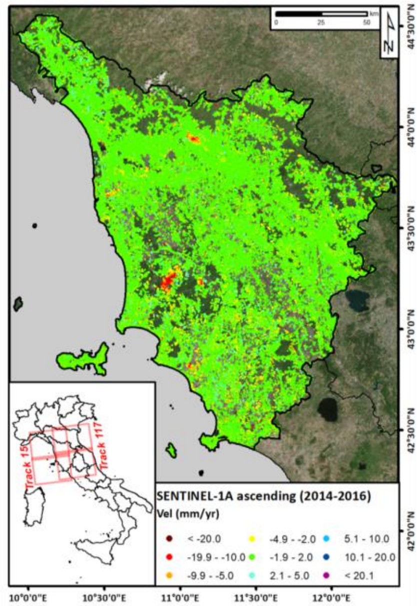

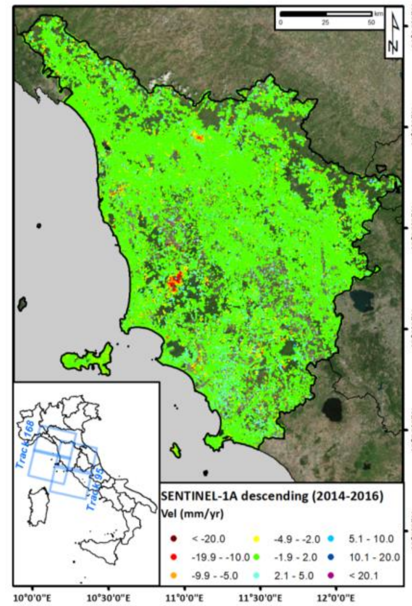

Structure	PS Mapping	PS Monitoring
Type	Single product	Continuous service
Time	deferred	real
Update	1 year	6 days
Aim	Update of landslides inventory maps	Update of scenarios for geohazard risks

Displacement rate >10 mm/yr

Ascending geometry

Ground deformation maps

Velocity filtering

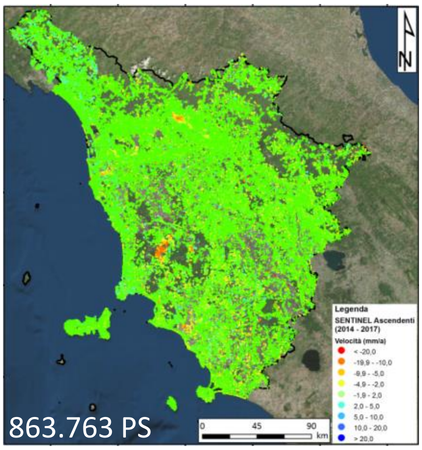

10 mm/yr →

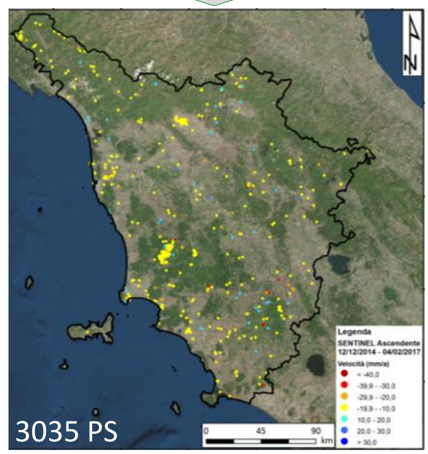

Displacement rate >10 mm/yr

Descending geometry

Ground deformation maps

Velocity filtering

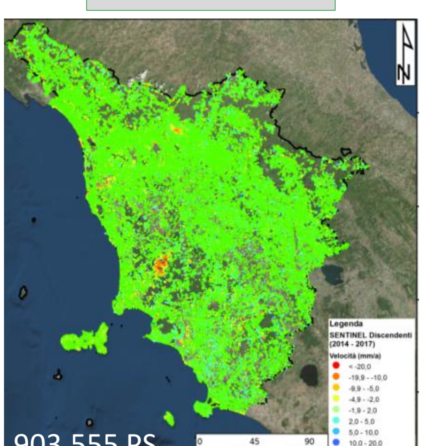

10 mm/yr →

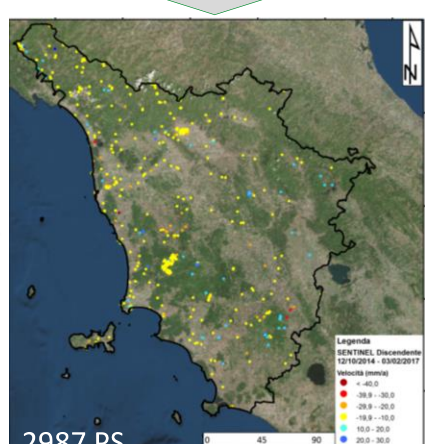

PSI Hotspot and Clustering Analysis (PSI-HCA)

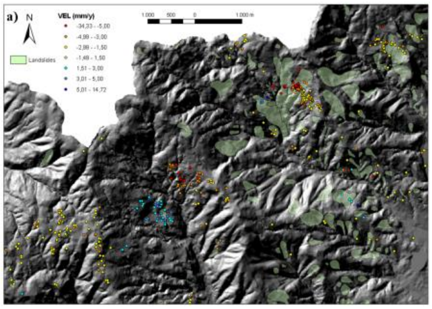

Scattered PS

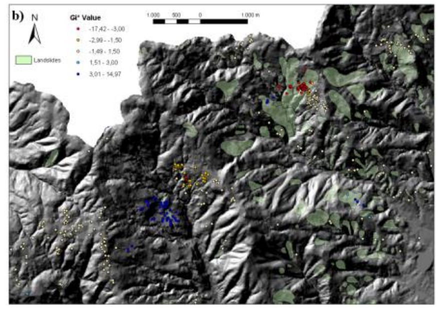

Clustered PS

1. Getis-Ord G_i* Statistics $$G_i^*(d) = \frac{\sum_j w_{ij}(d)x_j - W_i^* \bar{x}^*}{s^* \{[(nS_{1i}^*) - W_i^{*2}]/(n-1)\}^{0.5}}$$
2. Kernel density estimation $$f(x) = \frac{1}{nh}\sum_{i=1}^{n} K(\frac{x-X_i}{h})$$

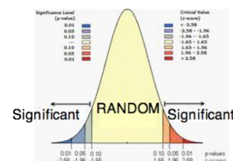

Ping et al. (2011) - International Journal of Remote Sensing

Automatic Hotspot detection

PSI Hotspot and Clustering Analysis (PSI-HCA)

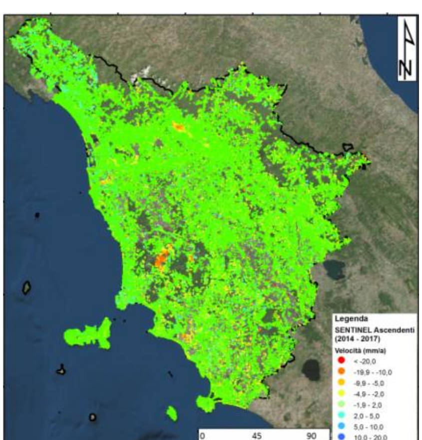

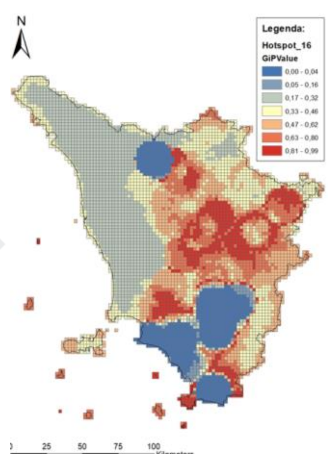

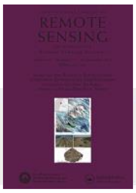

Journal
International Journal of Remote Sensing ›
Volume 33, 2012 - Issue 2

Original Articles

Persistent Scatterers Interferometry Hotspot and Cluster Analysis (PSI-HCA) for detection of extremely slow-moving landslides

Ping Lu, Nicola Casagli, Filippo Catani & Veronica Tofani

Pages 466-489 | Received 07 Dec 2009, Accepted 08 Mar 2010, Published online: 02 Nov 2011
Download citation https://doi.org/10.1080/01431161.2010.536185

PS mapping results

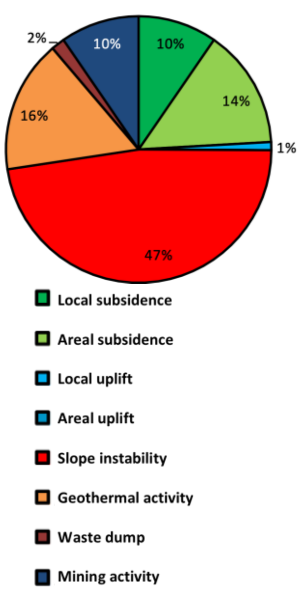

Province	AS	LS	LU	AU	SI	GA	WD	MA	Total
Pisa	10	3	0	0	8	36	0	7	64
Grosseto	9	5	1	0	24	10	3	8	60
Massa Carrara	0	0	0	0	37	0	0	3	40
Pistoia	15	1	1	0	10	0	0	0	27
Firenze	1	6	0	0	16	0	0	3	26
Siena	0	2	0	0	18	3	0	2	25
Livorno	8	10	1	0	1	0	0	5	25
Arezzo	0	2	0	0	15	0	2	2	21
Lucca	1	0	0	0	10	0	0	1	12
Prato	0	0	0	0	3	0	0	0	3
Total	44	29	3	0	142	49	5	31	**303**

Risk ranking

Cluster of deformation and elements at risk

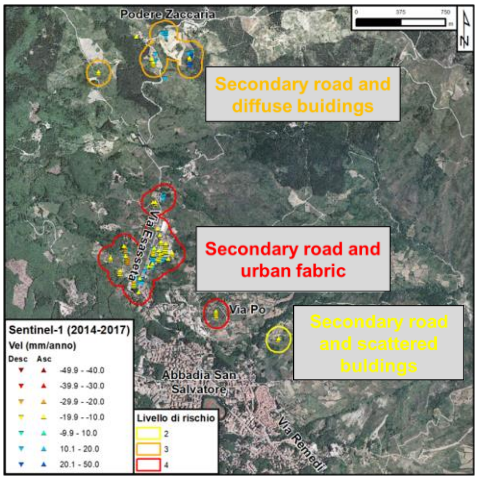

Abbadia San Salvatore (SI)

Class	Description
1	No clusters of deformation
2	Scattered elements at risk within the cluster of deformation
3	Diffused elements at risk within the cluster of deformation
4	Urban areas within the cluster of deformation

Risk ranking

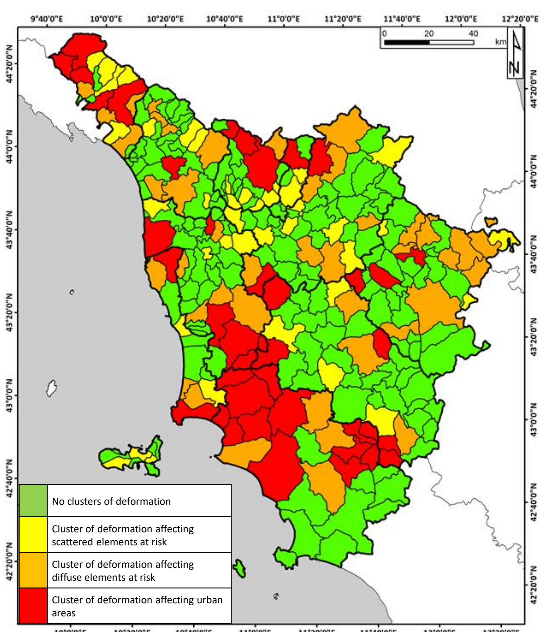

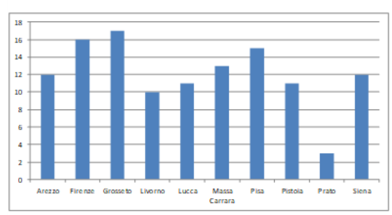

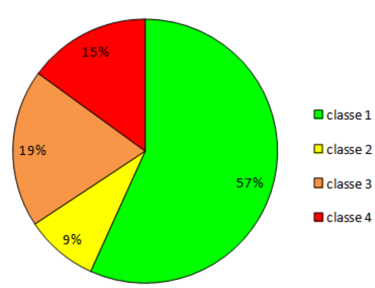

Validation field surveys: Abbadia (Siena)

Validation field surveys: Abbadia (Siena)

PS Monitoring

Capturing changes in the deformation pattern through time

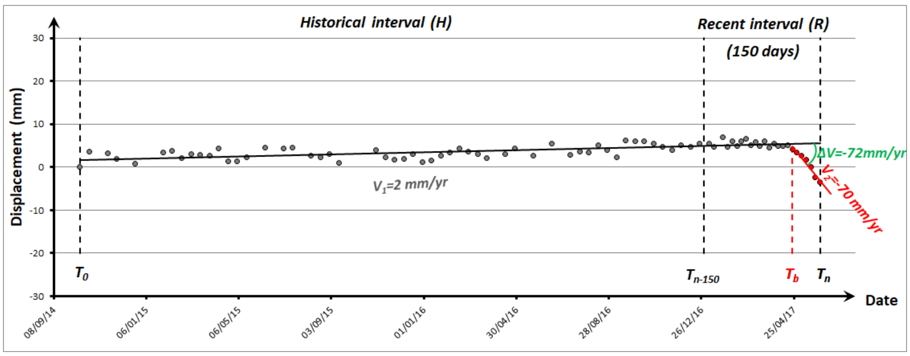

Identification of trend changes within the last 150 days in the displacement time series. An anomalous point is automatically highlighted as the difference between the deformation velocities (|ΔV|) recorded in the two-time intervals (T_0-T_b and T_b-T_n) is > 10 mm/yr.

Types of anomaly

Accelerating negative

Accelerating positive

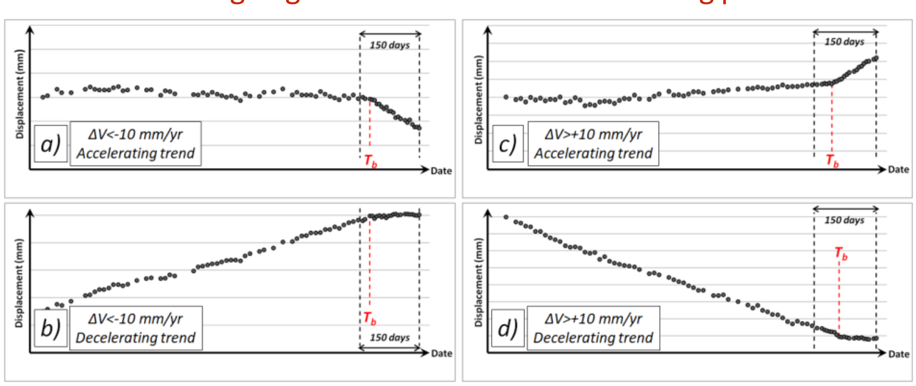

Decelerating negative

Decelerating positive

Field check

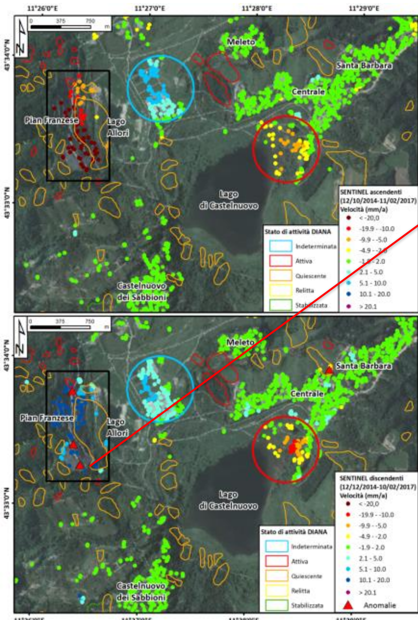

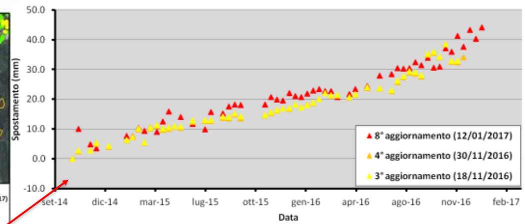

Validation field surveys

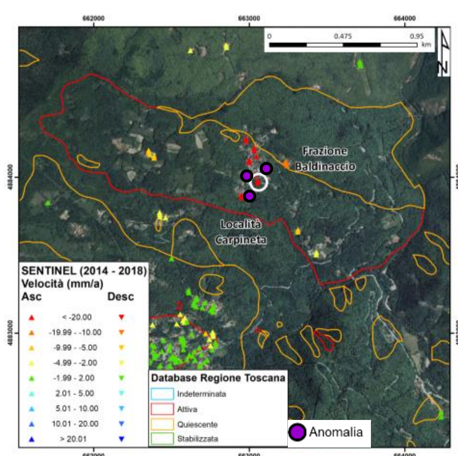

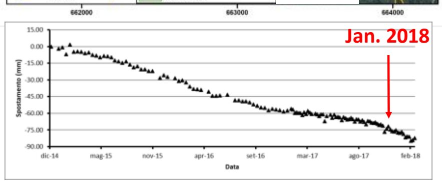

Sambuca Pistoiese (Pistoia)

Landslides

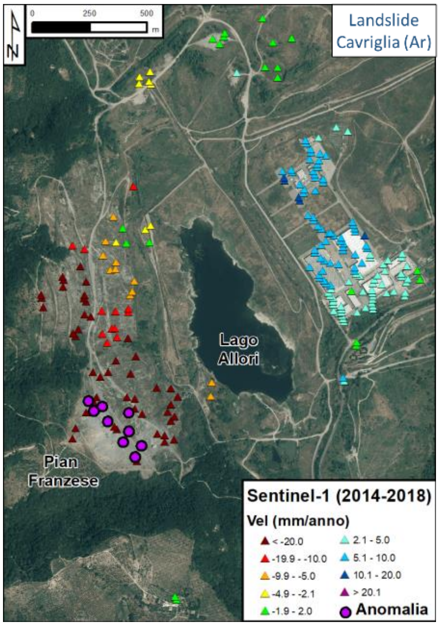

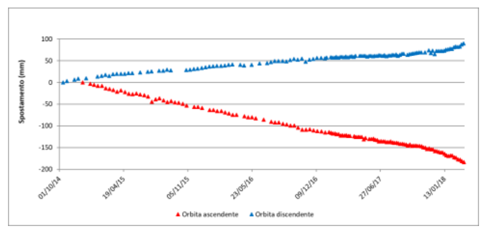

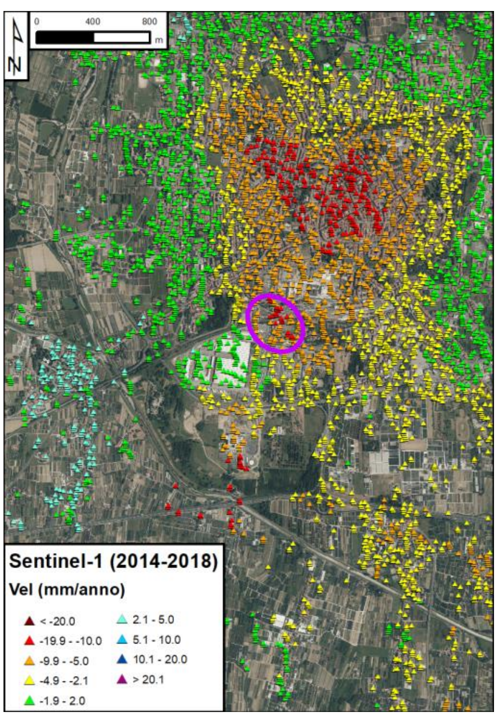

Subsidence

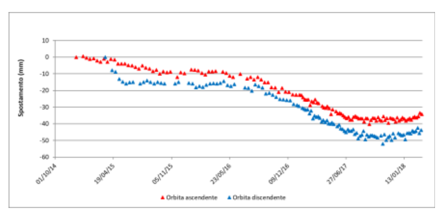

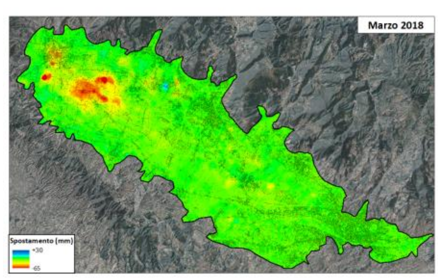

Mining activity

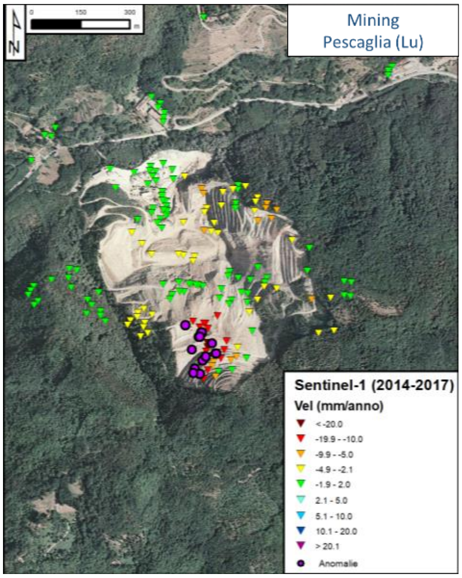

Levee instability

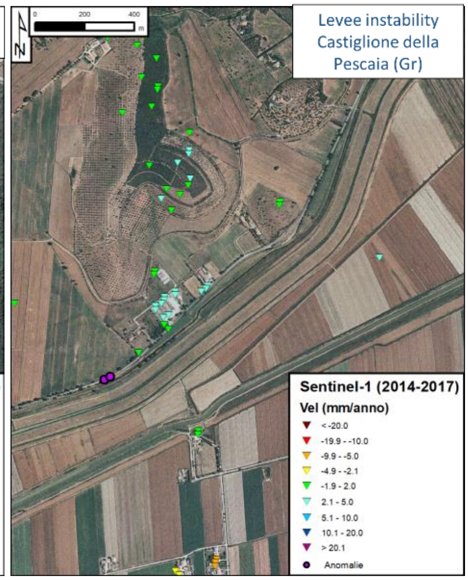

Uplift

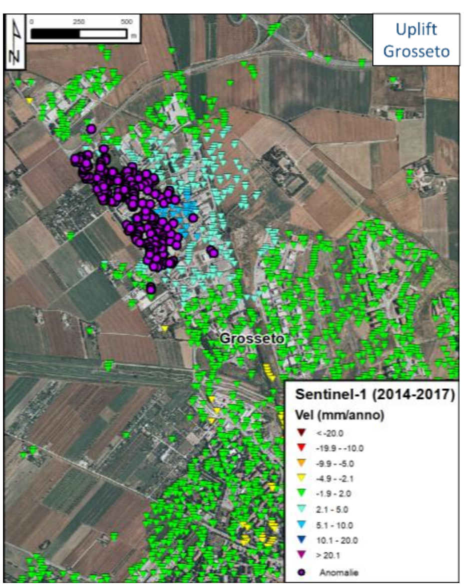

Geothermal activity

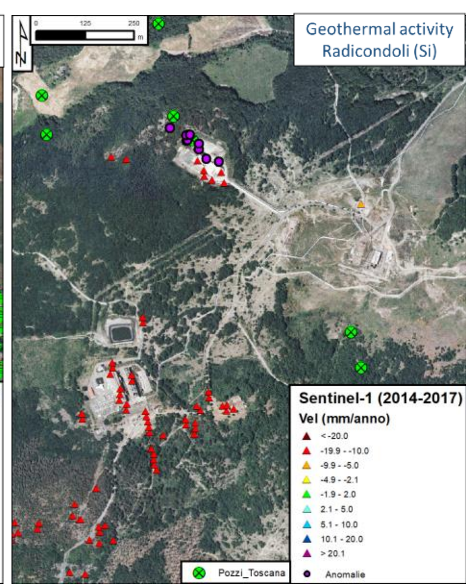

Causes of the anomalies

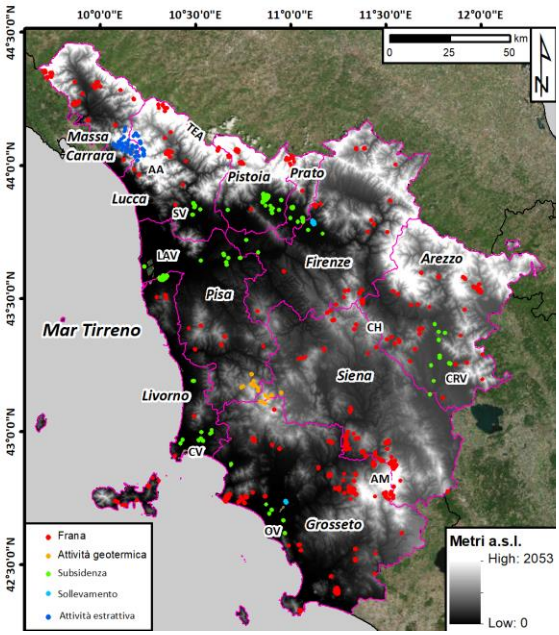

Cause	%
Subsidence (Local and areal)	64.74
Slope instability	29.58
Uplift (Local and areal)	3.5
Mining activity	1.63
Geothermal activity	0.48
Levee instability	0.05
Landfills	0.02

Monitoring bulletins

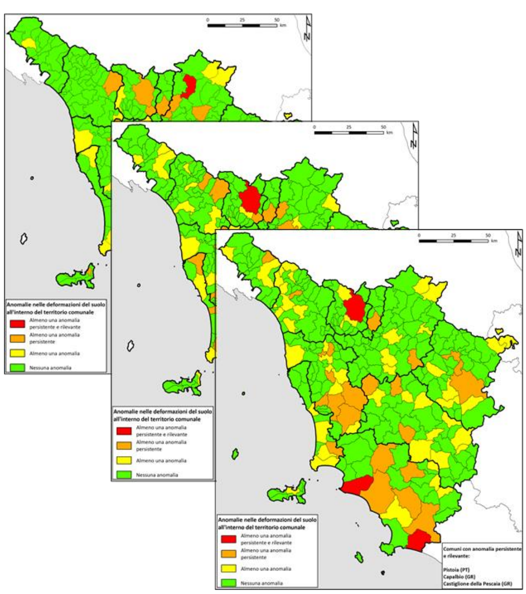

Class	Description
1	No anomaly within the municipality
2	At least one anomaly within the municipality
3	At least one persistent anomaly within the municipality
4	At least one persistent and relevant anomaly within the municipality

nature

www.nature.com/scientificreports

SCIENTIFIC REPORTS

OPEN

Continuous, semi-automatic monitoring of ground deformation using Sentinel-1 satellites

Received: 24 November 2017
Accepted: 17 April 2018
Published online: 08 May 2018

Federico Raspini[1], Silvia Bianchini[1], Andrea Ciampalini[1,3], Matteo Del Soldato[1], Lorenzo Solari[1], Fabrizio Novali[2], Sara Del Conte[2], Alessio Rucci[2], Alessandro Ferretti[2] & Nicola Casagli[1]

We present the continuous monitoring of ground deformation at regional scale using ESA (European Space Agency) Sentinel-1constellation of satellites. We discuss this operational monitoring service through the case study of the Tuscany Region (Central Italy), selected due to its peculiar geological setting prone to ground instability phenomena. We set up a systematic processing chain of Sentinel-1 acquisitions to create continuously updated ground deformation data to mark the transition from static satellite analysis, based on the analysis of archive images, to dynamic monitoring of ground displacement. Displacement time series, systematically updated with the most recent available Sentinel-1 acquisition, are analysed to identify anomalous points (*i.e.*, points where a change in the dynamic of motion is occurring). The presence of a cluster of persistent anomalies affecting elements at risk determines a significant level of risk, with the necessity of further analysis. Here, we show that the Sentinel-1 constellation can be used for continuous and systematic tracking of ground deformation phenomena at the regional scale. Our results demonstrate how satellite data, acquired with short revisiting times and promptly processed, can contribute to the detection of changes in ground deformation patterns and can act as a key information layer for risk mitigation.

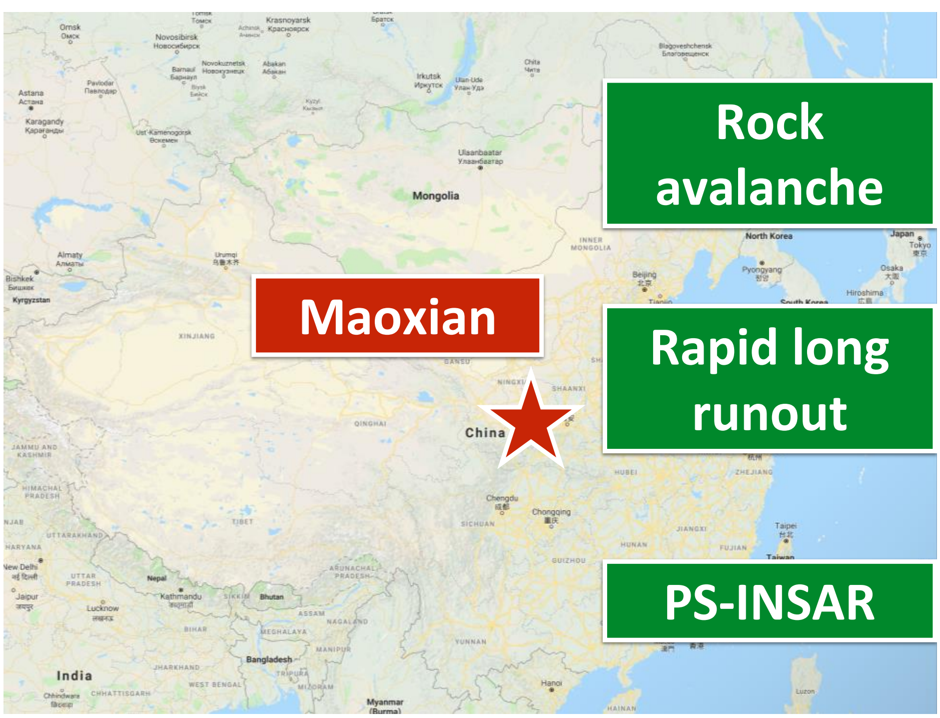

Maoxian landslide (China)

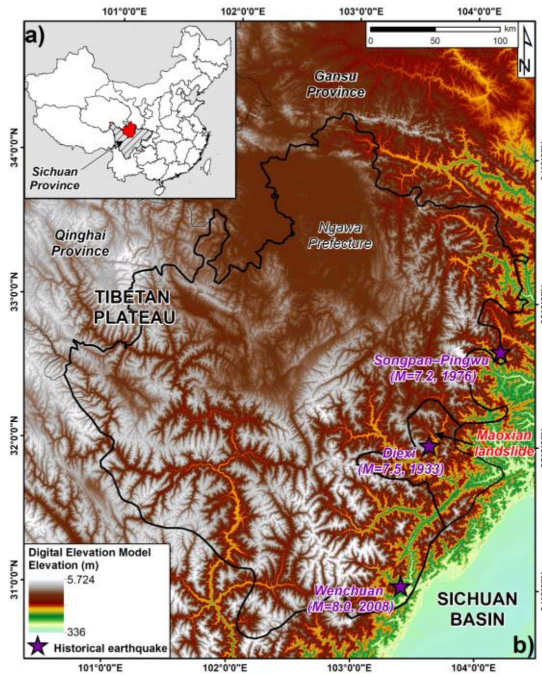

5 July 2017

240+ victims

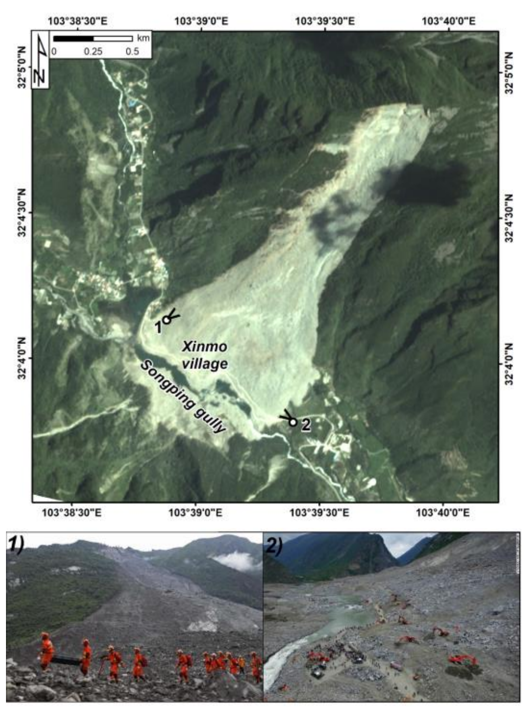

PS-Sentinel descending

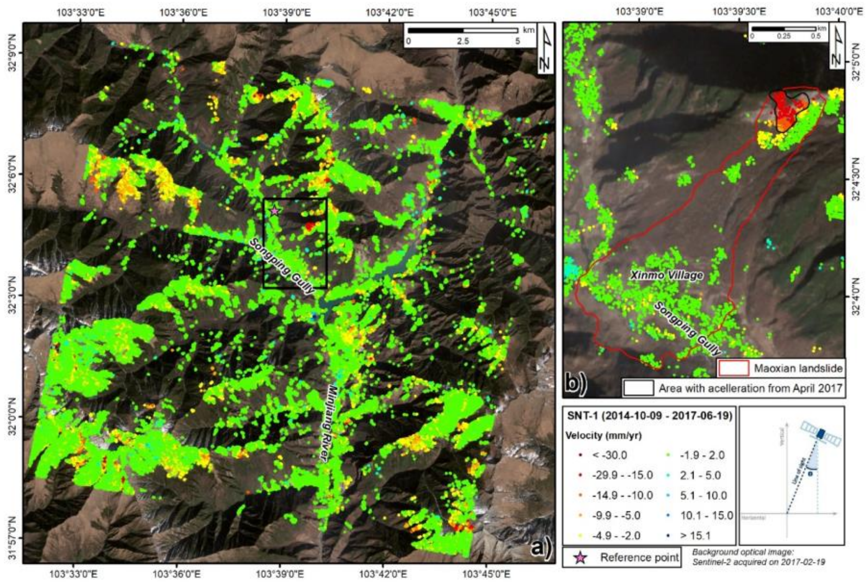

PS-Sentinel descending

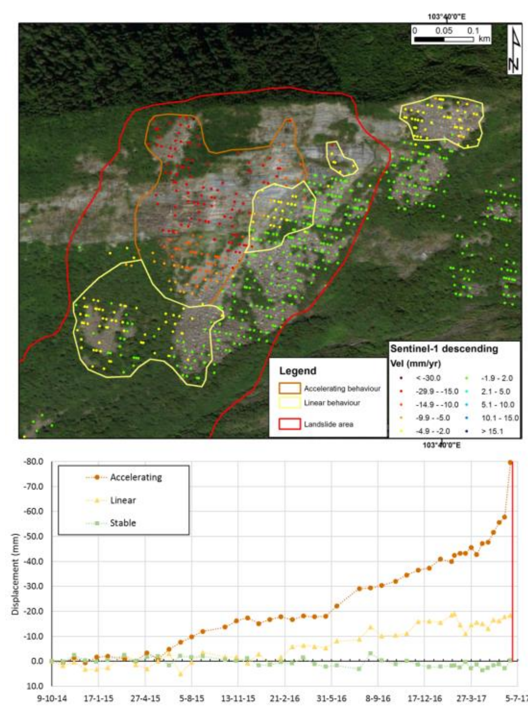

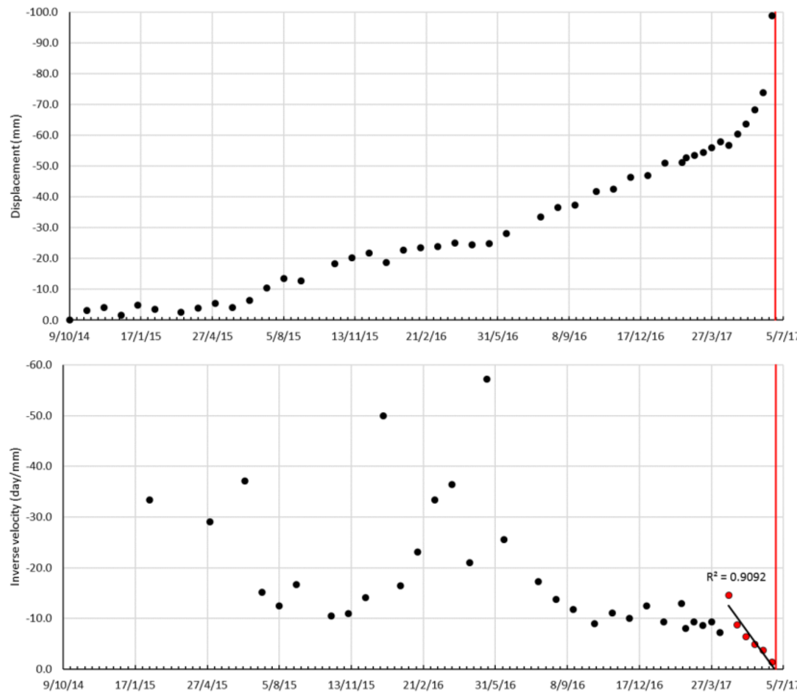

Landslides
January 2018, Volume 15, Issue 1, pp 123–133 | Cite as

The Maoxian landslide as seen from space: detecting precursors of failure with Sentinel-1 data

Authors Authors and affiliations

Emanuele Intrieri, Federico Raspini, Alfio Fumagalli, Ping Lu, Sara Del Conte, Paolo Farina, Jacopo Allievi, Alessandro Ferretti, Nicola Casagli

6th World Landslide Forum

6th WORLD LANDSLIDE FORUM
2023 FLORENCE ITALY

Follow us on:

protezionecivile.unifi.it

protezionecivile.unifi

UNIVERSITÀ DEGLI STUDI FIRENZE

PROTEZIONE CIVILE

@cpc_unifi